

Diverse classical walking of a single atom in an amplitude-modulated standing wave lattice

Lin Zhang,* H. Y. Kong, and S. X. Qu
*Institute of Theoretical and Computational Physics,
Shaanxi Normal University, Xi'an 710062, P. R. China*

(Dated: November 20, 2018)

The classical walking behaviors of a single atom in an amplitude-modulated standing wave lattice beyond the internal dynamics are investigated. Based on a simple effective model, we identify a diversity of dynamic regimes of atomic motion by periodically adjusting the lattice depth. Harmonic oscillation or pendulum rotation with classical step-jumping, random scattering walking, chaotic transportation, quasi-periodic trapped motion and roughly ballistic free flying are found in this simple model within different parametric regions by approximate analyses. Our study demonstrates a complex motion of single atom in modulating optical lattice beyond the quantum description.

PACS numbers: 05.45.Mt, 37.10.Jk, 05.40.-a, 37.10.Vz

I. INTRODUCTION

Nowadays, the fabrication technology steps more and more towards the atomic scale, and detection on one single molecular or atom is now an promising technique [1, 2]. Controlling one atom in the cavity quantum electrodynamics has now nearly met this step [3–5]. Based on this situation, the motion of one single atom in a controlled 1-dimensional (1D) optical lattice becomes a hot topic with a continuous interesting for its basic theoretical value and reliable applications in quantum information processing [6], atom lithography [7], solid state physics [8], quantum walking algorithm [9, 10], plasmonic application [11, 12], quantum-to-classical transition [13] and molecular dynamics. In the optical lattice, the atom can be accelerated [14] or decelerated [15] by an optical force for the purpose of precise control. However, in atomic scale, quantum effect starts to play a tricky role in the atomic dynamics. For example, under a deterministic linear force, the atomic motion is still beyond definite prediction in quantum theory because of an intrinsic uncertain variation. That the quantum motion distinguished from a classical trajectory motion is actually due to the superposition of the atomic wave packet which induces interference effect such as dynamical localization [16]. But, just for one single atom, the external wave superposition will be excluded [17] and the motion at different time, also, will not interfere unless a long memory imprinted on the optical field can feed back to the atomic motion along the classical trajectory. However this memory will also be cut down by a definite external optical control. Therefore the quantum motion and the classical motion meet together at this single atomic scale.

According to quantum descriptions by including internal level transitions, many kinds of motional behaviors were found in this single atomic system, such as nonclassical motional states, ballistic transport, harmonic oscillations, random walks, Lévy flights, and chaotic transport [18–23]. Which of these behaviors are derived from quantum description and which comes from classical dynamics are still a mixing problem in this system. This multiple dynamics inspires us to find if there exists a simple classical model without internal dynamics to reproduce most of the above dynamical processes. The interesting thing is that, in this paper, we do find a simple classical model which can produce most of above behaviors without directly considering internal dynamics. We identify a rich dynamic picture of the atomic motion in this classical model in order to pick up all the classical information from a mixture of description. Our study is not to give differences between quantum dynamics and classical dynamics because different descriptions will definitely give different results such as using different phase-space distribution functions [24]. The only thing to do, in this paper, is to find out all the classical dynamics of atomic walking within a classical framework and make a try to show whether some nonclassical motions are more a classical collective behavior (or a long time statistical behavior) than a quantum wave description of an individual particle. In order to give a full picture of the classical motion for a quantum system easy for check, we closely investigate the classical walking of a single atom in a controlled optical lattice. We first derive the simple classical dynamic model in section II, and find out a variety of atomic walking behaviors of the model in section III. Some approximate analytical solutions on specific conditions are given to understand the complicated behaviors of atomic walking in this unsolvable system. Section IV provides the simple discussions and the main conclusions.

*Electronic address: zhanglincn@snnu.edu.cn

II. THE SIMPLE CLASSICAL MODEL

What we start with is a widely verified quantum model which describes the dipole interaction between an atom and a classical field named Rabi model [25]. The dynamic of a two-level atom with a dipole moment \mathbf{d} interacting with a quasi-monochromatic plane-wave field,

$$\mathbf{E}(\mathbf{r}, t) = \mathbf{e}_\lambda \mathcal{E}(\mathbf{r}, t) \cos(\nu t - \mathbf{k} \cdot \mathbf{r}), \quad (1)$$

is described by a Hamiltonian of

$$\hat{H} = \frac{\hat{\mathbf{p}}^2}{2m} + \frac{1}{2} \hbar \omega_0 \hat{\sigma}_z - \hbar \Omega(\mathbf{r}, t) \cos(\nu t - \mathbf{k} \cdot \mathbf{r}) (\hat{\sigma}^- + \hat{\sigma}^+), \quad (2)$$

where the Rabi frequency is defined by $\Omega(\mathbf{r}, t) = \mathcal{E}(\mathbf{r}, t) \cdot \mathbf{d}/\hbar$. In Eq.(1), $\mathcal{E}(\mathbf{r}, t)$ is the temporal envelop of the wave field which can be definitely controlled in the experiment. The modulated Rabi frequency $\Omega(\mathbf{r}, t)$ expresses the coupling intensity of the field mode with the atomic dipole \mathbf{d} , and $\hat{\sigma}^+$ ($\hat{\sigma}^-$) is the atomic level raising (lowering) operator. Hamiltonian (2) is a widely used model to study the interaction between a two-level atom and a classical field with different controlling modes denoted by $\Omega(\mathbf{r}, t)$.

However, what we consider here is a simple case: a single atom interacts with a standing wave mode in a microcavity with only its axial direction, x , getting involved. In this case, the Hamiltonian becomes

$$\hat{H} = \frac{\hat{p}^2}{2m} + \frac{1}{2} \hbar \omega_0 \hat{\sigma}_z - \hbar \Omega(x, t) \cos \nu t (\hat{\sigma}^- + \hat{\sigma}^+), \quad (3)$$

where $\Omega(x, t)$ depends on the axial cavity-mode with an envelop modulated by the input field. In a resonant mode field, Eq.(3) reduces to a so-called double resonance model [26] with an effective Hamiltonian of (see Appendix A for details)

$$\hat{H} = \frac{\hat{p}^2}{2m} - \hbar \lambda \cos(\chi t) \cos(k\hat{x}), \quad (4)$$

where the key parameter χ is the modulation frequency of the field amplitude. Eq.(4) is an extensively considered model [27–30] along with the phase-modulated model [31] in quantum chaos. Here the Hamiltonian describes the dynamics of an atom (or a polar molecule) moving in an amplitude-modulated standing wave under an effective coupling constant λ . However in quantum theory, this model is time-dependent and difficult to be solved in a normal technique [32]. For one single atom, we can introduce the following dimensionless classical variables $H = \langle \hat{H} \rangle / \hbar \omega_r$, $p = \langle \hat{p} \rangle / \hbar k$, $x = k \langle \hat{x} \rangle$, and dimensionless parameters $\lambda' = \lambda / \omega_r$, $\omega = \chi / \omega_r$, $t' = \omega_r t$, scaled by recoil frequency of a single photon $\omega_r = \hbar k^2 / m$. The label $\langle \hat{O} \rangle = O$ means the expectation value of the corresponding quantum operator \hat{O} and this is a very good approximation for one single atom. In atomic scale, a single atom can be treated as a classical point with its position identified by the center of mass, and no fluctuations induced by spatial superposition exist here. Therefore the classical model can be obtained (primes are omitted) by

$$H(t) = \frac{p^2}{2} - \lambda \cos x \cos \omega t. \quad (5)$$

According to Eq.(5), the classical dynamic equations are

$$\dot{x} = \frac{\partial H}{\partial p} = p, \quad \dot{p} = -\frac{\partial H}{\partial x} = -\lambda \sin x \cos \omega t, \quad (6)$$

or

$$\ddot{x} + \lambda \cos \omega t \sin x = 0. \quad (7)$$

Eq.(7) looks simple, but it is a time-dependent nonlinear differential equation and no closed analytical solution for an arbitrary parameter is available [33].

The steady solutions of Eq.(7) are clear at the antinode sites for $x^* = 0, \pm\pi, \pm 2\pi, \dots$ and $p^* = 0$, but they are not always stable because the trapping potential is time-dependent in the way of

$$V(x, t) = -\lambda \cos(\omega t) \cos x = -\frac{\lambda}{2} [\cos(x + \omega t) + \cos(x - \omega t)],$$

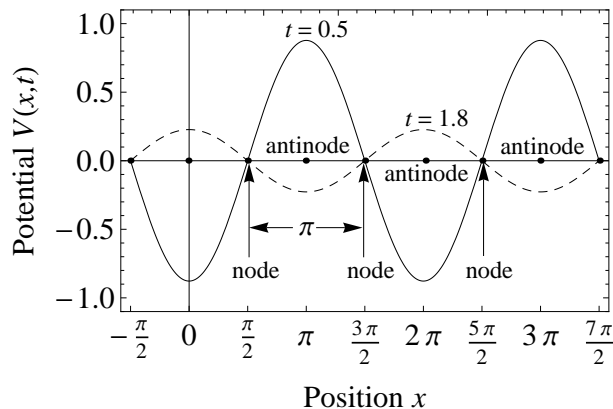


FIG. 1: The effective potential along lattice x at different time $t = 0.5$ (solid line) and $t = 1.8$ (dashed line) with parameters $\lambda = 1, \omega = 1$. The time t is scaled by recoil frequency ω_r and the position x is scaled by the wavelength of the cavity mode.

which acts on the atom as a superposition of two potential waves propagating in opposite directions. In a high fineness cavity, this potential is usually used to control atomic motion and can be easily generated by a modulation of standing cavity-mode. Fig.1 shows the varying potentials at two different times along the axial direction. The nodes (indicated by arrows) or antinodes of the potential lattice are fixed with a spatial period of π but the amplitude of the lattice wave changes with time with a period of $t = 2\pi/\omega$. The amplitude λ at antinodes denotes the atom-lattice coupling indicating a trapping ability of the atom at antinode, so we can call it as a lattice depth. All the above lattice parameters can influence the dynamic of the atom and all can be controlled by an external optical field.

However, due to atomic motion, the potential lattice felt by the atom also depends on the momentum of the atom. If we suppose that the velocity of the atom is a slowly varying quantity during a time period of $[0, t]$, we can set

$$x(t) = \int_0^t p(\tau) d\tau = \langle p \rangle \cdot t \approx p_0 \cdot t,$$

where $\langle p \rangle$ is a time average of momentum which can be replaced by its initial value of p_0 . In this case, the optical force will be

$$F(t) = -\frac{\partial V}{\partial x} = -\frac{\lambda}{2} [\sin(\omega + p_0)t - \sin(\omega - p_0)t], \quad (8)$$

which clearly indicates that there are two driven forces exerted on the atom with two different frequencies depending on atomic momentum, suggesting two nonlinear resonance points of the dynamics at $\omega \pm p_0$ [26]. Therefore, the motion of the atom across the varying lattice field is dependent on two aspects: the lattice field and the state of the atom. Although this model described by Eq.(5) is simple, it can display most of the dynamic behaviors found in [19–23] without directly including the internal dynamics.

III. DIVERSITY OF WALKING BEHAVIOR

A. Oscillation with random step-jumping

Under the condition that the amplitude of the lattice is varying slowly, the cold atom ($p < 2\sqrt{\lambda}$) will be trapped at the bottom of the lattice potential for a long time, oscillating around the antinodes at $\sin x^* = 0$, i.e. $x^* = \pm n\pi, n = 0, 1, 2 \dots$. In Fig.2, a typical walking process of this case is shown by a numerical simulation on Eq.(6). Fig.2(a) displays a temporal position (black line) and momentum (gray line) of the atomic walking and Fig.2(b) is its orbit in the phase space. We can see that the atom first oscillates around one of antinodes (indicated by the horizontal dashed lines) and then jumps randomly in an integer steps of π to a left or right antinode after a time interval of π/ω . The random atomic jumping to a new site is due to the loss of stability of the former site when the coupling intensity $\lambda(t) = \lambda \cos(\omega t)$ turns from positive to negative. This classical jumping behavior demonstrated in this model will reversely affect the lattice field and can be traced by the transmission field from the cavity due to a motion-dependent detuning effect [34, 35]. Although a similar dynamic behavior was revealed by Domokos and

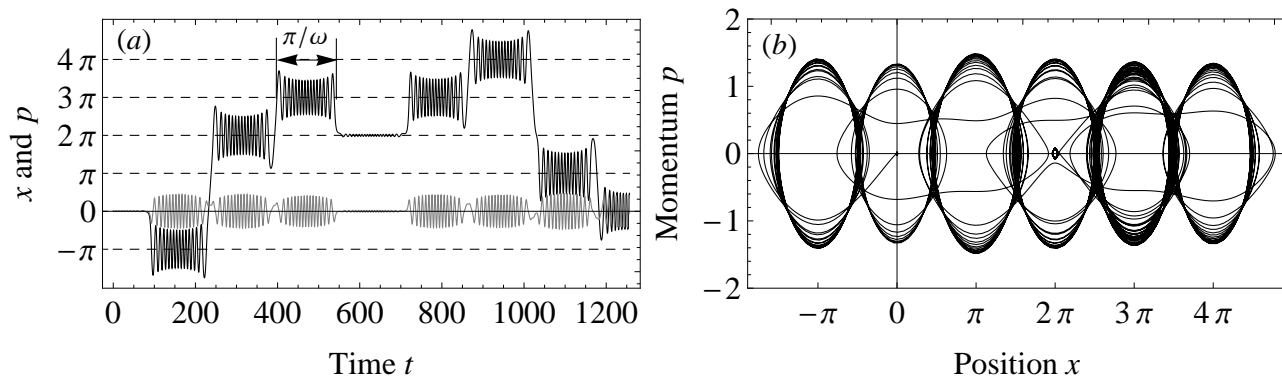


FIG. 2: A typical walking trajectory of a cold atom in slowly varying standing wave with $\lambda = 1$, $\omega = 0.02$, the initial position and momentum $x_0 = 0$, $p_0 = 0.02$. (a) The evolution of the atomic position (black line) and momentum (gray line). (b) The corresponding orbit in phase space.

Ritsch [36], the mechanisms of two systems are different. Our system is only for one single atom and no random Langevin-type noise is necessary during the dynamics. In order to understand more about this classical trapping and jumping behavior, we can analyze it by the following extreme approximations.

1. Harmonic Oscillation with random jumping

For the small modulation frequency of $\omega \ll 1$, the approximation of $\cos \omega t \sim 1$ is valid for a short time. The linearization for a cold atom ($p \ll \sqrt{\lambda}$ for tightly trapping) around the stable positions of $\sin x^* = 0$, such as $\sin x \sim x$ around 0 (for other site we can set $x' = x - x^*$) can be used here. Then Eq.(7) will reduce to

$$\ddot{x} + \lambda x \approx 0, \quad \omega \ll 1, \quad (9)$$

where we set $\lambda > 0$ and this enables Eq.(9) a harmonic oscillation solution of

$$x(t) \approx x(0) \cos(\sqrt{\lambda}t) + \frac{p(0)}{\sqrt{\lambda}} \sin(\sqrt{\lambda}t), \quad (10)$$

which describes a main properties of atomic walking in this case. Eq.(10) indicates that the oscillation frequency in Fig.2(a) is determined by the depth of the trap, λ , and gives an important characteristic time of oscillation period, $2\pi/\sqrt{\lambda}$. As the temporal depth $\lambda(t) = \lambda \cos \omega t$ changes slowly with time, the oscillation frequency will adiabatically follow with $\sqrt{\lambda(t)}$. When $\lambda(t)$ becomes negative, the oscillation frequency $\sqrt{\lambda(t)} \rightarrow i\sqrt{|\lambda(t)|}$, and the atom will escape exponentially from the former site in a way of

$$x(t) \approx x(0) \cosh(\sqrt{\lambda}t) + \frac{p(0)}{\sqrt{\lambda}} \sinh(\sqrt{\lambda}t). \quad (11)$$

Therefore the atom will conduct an oscillation followed by an escaping jump from the former site. In order to see the details of this motion, Fig.3(a) exhibits a zoomed in orbit around one antinode in phase space. The black line is the real orbit and the thick gray ellipse stands for the harmonic oscillation of Eq.(10), where the potential lattices at time $t = 0$ and at the end of one oscillation $t = 27\pi$ are depicted by the dashed lines for reference. As a decrease of $\lambda(t)$, the elliptic orbit in the phase space expands along x until $\lambda(t)$ decreases to a value that the atom can pass through it to another site at a location determined by the escaping momentum. Therefore the trapping time around antinodes for the cold atom is about π/ω as indicated in Fig.2(a), which is estimated by the time when $\lambda(t)$ changes from positive value to negative value. In Fig.3(a), the oscillating time of the atom around the starting site is about $t = \pi/2\omega = 25\pi$, which is just the time taking by the trap depth $\lambda(t)$ decreasing from maximum to zero.

Certainly, for a more rigorous approximation in above case of $\omega t \ll 1$, the time dependent part will be $\cos(\omega t) \approx 1 - (\omega t)^2/2$, and the atomic motion can be better described by a parabolic cylinder function satisfying differential equation of

$$\ddot{x} + \lambda(1 - \frac{\omega^2 t^2}{2})x = 0, \quad (12)$$

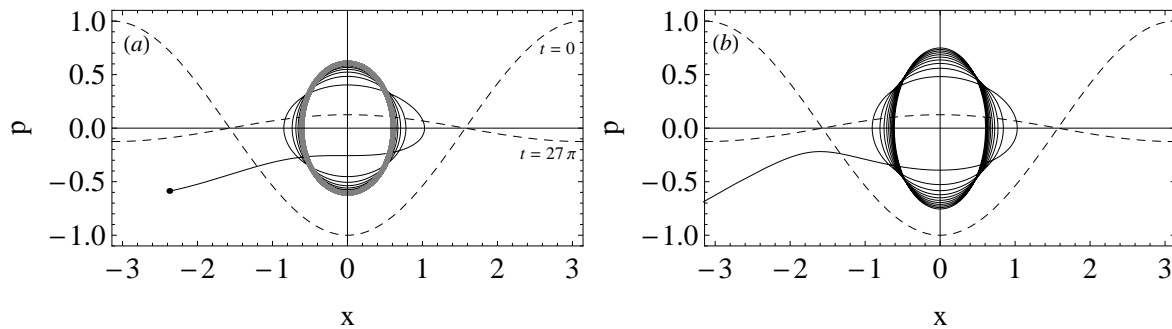


FIG. 3: The enlarged orbit of a cold atom in phase space with $\omega = 0.02$ and $\lambda = 1$. The initial position and momentum are $x_0 = 0.6$, $p_0 = 0.1$. (a) The orbit of the rigid simulation (solid black line) with harmonic approximation (gray thick line); (b) The approximation orbit of Airy solution of Eq.(13).

or even by an Airy function determined by

$$\ddot{x} + \lambda\left(\frac{\pi}{2} - \omega t\right)x = 0, \quad (13)$$

where the time approximation $\cos(\omega t) = \sin(\pi/2 - \omega t) \approx \pi/2 - \omega t$ is used. Fig.3(b) demonstrates a better orbit of the Airy solution than a harmonic oscillation at a short time. But for a longer time the dynamic will dramatically deviate from the real orbit because of a divergence of Airy function.

2. Pendulum rotation with random step-shifting

When varying frequency ω increases near to the oscillation frequency $\omega \sim \sqrt{\lambda}/2$, the trapping time π/ω of the cold atom will decrease and the atom will quickly shift from one site to another like a pendulum swinging or rotating around different equilibrium sites just for a few periods. As the motion of atom covers a large range of x relative to stable antinodes in this case, the spatial linearized Eq.(9) will be invalid. Therefore Eq.(7) should be

$$\ddot{x} + \lambda \sin x = 0,$$

which is the well-known pendulum equation with $\lambda > 0$. Actually, this situation corresponds to an atom moving in a

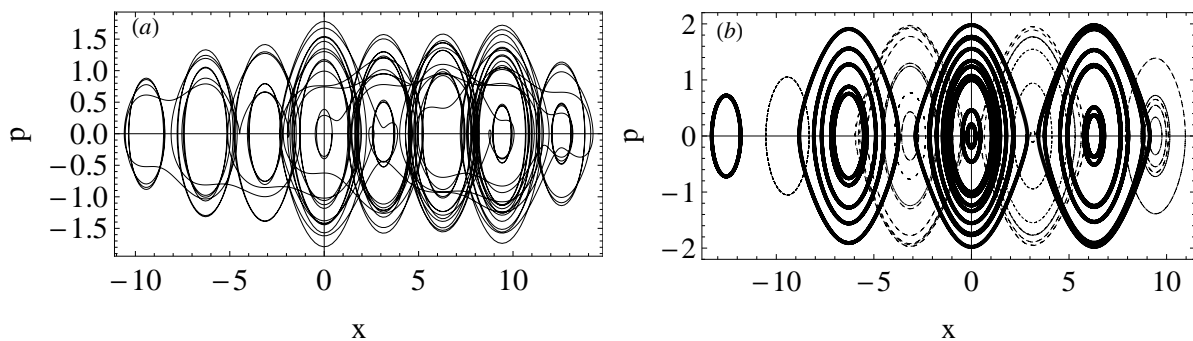


FIG. 4: The phase space picture of a cold atom walking in a slowly varying field with $\lambda = 1$, $\omega = 0.1$ and the initial atomic momentum $p(0) = 0$. (a) The rigorous solution for initial position being $x(0) = 0.4$; (b) The pendulum solution of Eq.(14) by using a random step-shifting (step unit π) position of Gaussian distribution with mean value of 0.4 and variance of $\pi/2$.

stationary one-dimensional lattice. When $\lambda > 0$, the integral solution of above equation takes the form of

$$x(t) = 2 \arcsin \left[\sin \frac{x_0}{2} SN \left(\sqrt{\lambda} t + K \left(\sin \frac{x_0}{2} \right), \sin \frac{x_0}{2} \right) \right], \quad (14)$$

with the initial conditions of $x(0) = x_0, \dot{x}(0) = 0$. The label $SN(\cdot, \cdot)$ is the Jacobi elliptic function and $K(\cdot)$ is the complete elliptic integral of the first kind defined by the elliptic integral of

$$K(k) = \int_0^{\pi/2} \frac{d\theta}{\sqrt{1 - k^2 \sin^2 \theta}}.$$

Walking orbits in the optical lattice with a higher modulation frequency $\omega = 0.1$ are demonstrated in Fig.4. Fig.4(a) is a rigid simulation and Fig.4(b) presents a pendulum samples of phase picture with random initial positions. We can see the long-time atomic walking can be somehow (not exactly) explained by the pendulum solutions with shifting equilibrium positions. As effective $\lambda(t)$ is actually time-dependent, the length of the pendulum will change gradually from positive to negative. When $\lambda(t) < 0$, the stable site at $x^* = 0, \pm 2\pi, \pm 4\pi, \dots$ for $\lambda(t) > 0$ will become unstable and shift to a new stable site at $x^* = \pm\pi, \pm 3\pi, \dots$, which is clearly shown in Fig.2(a) with a sequence of $-\pi, 2\pi, 3\pi, 2\pi, 3\pi, 4\pi, \pi, 0\pi, \dots$. In Fig.4(b) the thick black lines are pendulum solutions of Eq.(14) for $\lambda > 0$ and the thin dashed lines are for $\lambda < 0$. We use a Gaussian random number to pick up initial positions for the pendulum solutions and the results reveal that a long time atomic walking in Fig.4(a) can be illustrated by Eq.(14) with a random shifting of equilibrium position of pendulum rotation. The simulation indicates that this behavior is a combination of pendulum oscillation with a random shifting of the optical lattice.

According to above analysis, we can conclude that, in a slowly modulating optical lattice, the cold atom will feel a gradually changing wave trap, resulting in a harmonic or pendulum rotation followed by a random step-shifting. In this process, two characteristic times are important, trapping time π/ω and oscillation period $2\pi/\sqrt{\lambda}$. In addition, the step-shifting between antinodes of the lattice has a random characteristic and can not be predicted because the jumping process is very sensitive to position and momentum. In this respect, the atomic walking in modulated standing wave is very similar to one-dimensional billiard problem that a minor deviation of position (or momentum) will leads to a dramatically different walking orbit. However, above conclusion is on the conditions that the optical lattice is slowly modulated and the atom is very cold. In the following parts we will find some other specific walking behaviors beyond these constraints.

B. Random walking and Chaotic transportation

When the modulation frequency of the lattice is further increased, the trapping time of the cold atom, π/ω , will decrease to an extent that it is comparable to the shifting time between different sites, $\pi/\langle p \rangle$ ($\langle p \rangle$ is average momentum during a walking interval). In this case, the atom will exhibit a random like walking that is shown in Fig.5(a) by

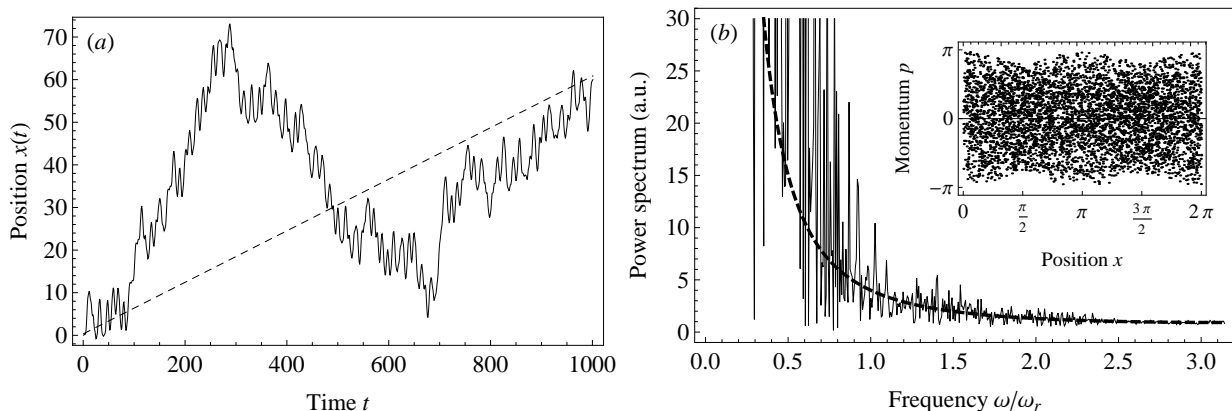


FIG. 5: (a) A typical random walking of a cold atom in varying standing field of $\omega = 0.8, \lambda = 2$ with $x(0) = 0, p(0) = 0.4$. The dashed line is the average motion of the atom. (b) The corresponding power spectrum of the random walking (solid) and the average motion (dashed). The inset picture is the phase-space distribution of the walking mapped to $[0, 2\pi]$.

a typical sample of moving sequence along optical lattice, displaying an unpredictable position of the atom in the periodically varying lattice. This random characteristic can be further verified by a power spectrum of this walking depicted in Fig.5(b). The dashed line in Fig.5(a) corresponds to the effective uniform motion of this walking with an average momentum of $\langle p(t) \rangle_T \approx 0.4 + 0.06$ (T is the total walking time), whose fourier spectrum is depicted by a thick dashed line for reference. The inset picture of Fig.5(b) is a long time phase-space distribution of the atom by mapping

its walking position into the first periodic region of the lattice $[0, 2\pi]$. The uniform phase-space distribution is a statistical proof of the random properties coming up in this deterministic system where regular and chaotic regions coexist in this walking process.

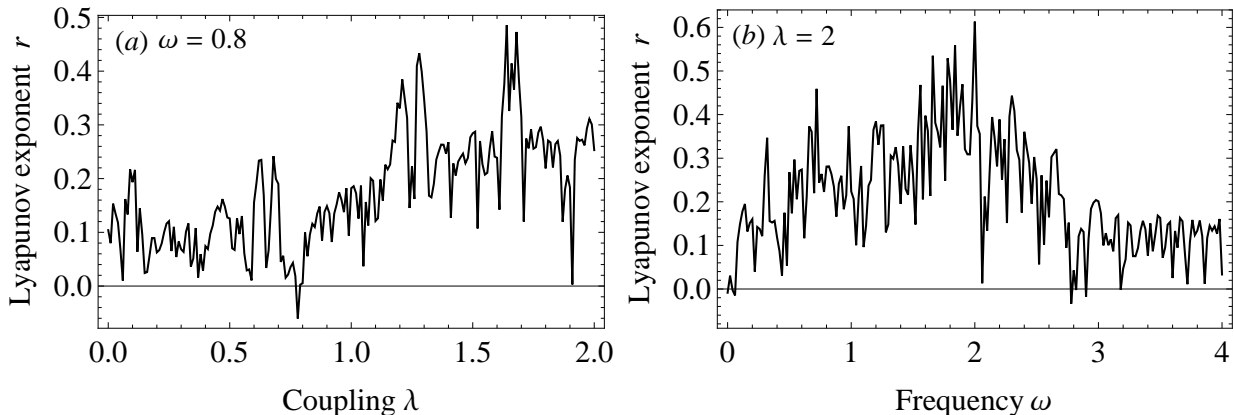


FIG. 6: (a) The Lyapunov exponent of the atomic walking versus coupling intensity λ with $\omega = 0.8$. (b) The Lyapunov exponent versus modulation frequency ω with $\lambda = 2$. The initial atomic position $x(0) = 0$, momentum $p(0) = 0.4$.

In the sense of walking sensitivity to the atomic state, above behavior can be treated as a chaotic transportation in the standing wave lattice similar to the results in [19, 23]. The estimation of Lyapunov exponents λ_i can give a rough analysis of this chaotic property. This system is equivalent to a 3-dimensional autonomous system with one Lyapunov exponent being zero (the third dimension is $\theta = \omega t$). Because the sum of the exponents for a Hamiltonian system is null, i.e., $\sum_i \lambda_i = 0$, therefore the Lyapunov exponents of this system must be $-r, 0, +r$. Fig.6 gives a rough estimate of the largest Lyapunov exponent r changing with the trapping depth λ (Fig.6(a)) and with the modulation frequency ω (Fig.6(b)), indicating a weak chaotic transportation along the standing wave lattice. The chaotic transportation of this system under the influence of internal transition has been investigated by Argonov and Prants [19, 20, 23], but our results reveal that only the external walking of an atom in a slowly varying optical lattice can present the similar chaotic behavior. Certainly, the similar fractal tunneling time [37] through a lattice with a certain length can also be found in this walking.

C. Quasi-periodic trapping state and its stability

In some parametric regions the atom will be totally trapped by the quickly varying standing wave. Fig.7(a) gives an example of this case when the frequency reaches to $\omega = 2.8\omega_r$ (left black bowknot orbit). In this case the atom takes a periodic or quasi-periodic oscillation around a stable site near initial position $x(0)$. In the following, we will give some detail analysis about this trapped walking behavior.

For an arbitrary varying frequency ω , Eq.(7) corresponds to a pendulum with changing length. The normal method of solving this nonlinear differential equation is the linearization approach. For the trapped atom that is very near to a stable antinode of $\sin x^* = 0$, for example, a small x near zero is $\sin x \sim x$, Eq.(7) will be reduced to

$$\ddot{x} + (\lambda \cos \omega t) x = 0, \quad (15)$$

which is a linear equation with a periodic coefficient and can be solved by Floquet's theorem [38]. The linearized equation (15) is a Mathieu equation

$$\frac{d^2 x}{dt^2} + [a - 2q \cos(2t)] x = 0$$

with a standard form of solution

$$x(t) = e^{i\mu t} X(t),$$

where μ , in general, is a complex function of a and q called characteristic exponent, and $X(t)$ is a periodic function. Explicitly, the solution of equation (15) reads

$$x(t) = x(0)C\left(0, -\frac{2\lambda}{\omega^2}, \frac{\omega t}{2}\right) + p(0)S\left(0, -\frac{2\lambda}{\omega^2}, \frac{\omega t}{2}\right), \quad (16)$$

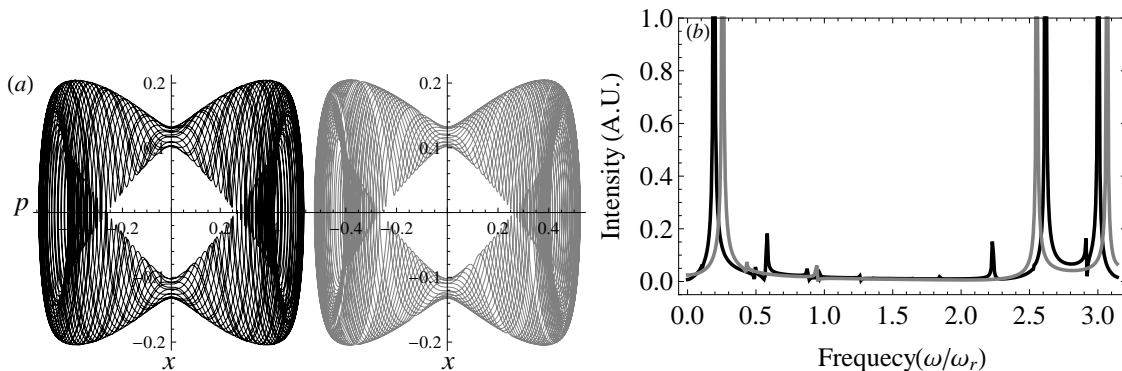


FIG. 7: (a) The phase portrait of strict solution of Eq.(7) (left black orbit) and the Mathieu solution of Eq.(16) (right gray orbit) with parameters $\lambda = 1, \omega = 2.8$ and the initial position and momentum being $x(0) = 0.2, p(0) = 0.18$. (b) The corresponding power spectrum of the atomic momentum for the strict solution (black line) and the Mathieu solution (gray line).

where $C(0, -\frac{2\lambda}{\omega^2}, \frac{\omega t}{2})$ and $S(0, -\frac{2\lambda}{\omega^2}, \frac{\omega t}{2})$ are Mathieu even and odd functions. Above solution can be used to estimate a variety of behavior of Eq.(7) under the trapping condition (for that the linearization condition is valid). Fig.7(a) is a comparison of Mathieu solution (right gray orbit) with the strict simulation (left black orbit) in phase space when Mathieu function is in its stable parametric region. The figures show a nice match of the linear approximation with Eq.(7) and the atom conducts a quasi-periodic oscillation around $x^* = 0, \pm\pi, \pm2\pi, \dots$. The quasi-periodic properties of this walking can be verified by the power spectrum of atomic momentum in Fig.7(b), where several frequency components are manifest but the atom never exactly repeat its walking orbit in the phase space. Certainly, on some parameters, the periodic walking is also available. This can be discussed by the characteristic exponent of Mathieu function. The characteristic exponent, $\mu(a, q) = \mu(0, -2\lambda/\omega^2)$, predicts that only for certain value of λ and ω can the solution be periodic. For parametric values of $2\lambda/\omega^2 > 0.91$, μ will be a complex number and Eq.(15) is unstable (see the borderlines $2\lambda/\omega^2 \approx \pm 0.91$ shown in Fig.8(a)). Therefore we can determine the stable or unstable parametric region of the linearization equation under independent initial conditions. However in the real system, the modulating amplitude will include a small constant part \mathcal{E}_0 [39] that is governed by

$$\frac{d^2x}{dt^2} + (\mathcal{E}_0 + \lambda \cos \omega t) x = 0,$$

and this enables a normal Mathieu solution of

$$x(t) = x(0)C\left(\frac{4\mathcal{E}_0}{\omega^2}, -\frac{2\lambda}{\omega^2}, \frac{\omega t}{2}\right) + p(0)S\left(\frac{4\mathcal{E}_0}{\omega^2}, -\frac{2\lambda}{\omega^2}, \frac{\omega t}{2}\right). \quad (17)$$

Fig.8 gives a stability diagram of solution Eq.(17) near stable positions x^* with the shaded area indicating stable region of the trapping states. Fig.8 shows an irregular stable parametric region of the walking determined by the lattice depth λ and the modulation frequency ω , with a symmetric structure for λ and a fractal boundary for small ω . Fig.8(b) also indicates that although the symmetric gap (indicated by the arrows in Fig.8(b)) of the stable region, $2\mathcal{E}_0$, in small frequency ω region goes to zero when $\mathcal{E}_0 \rightarrow 0$, the complicated structure of stable region will not disappear in Fig.8(a) for a real walking. This result reveals that the dynamic stability of atomic walking around antinodes in a varying lattice is very sensitive to the fluctuation of the optical field [30]. Actually the fluctuation of the lattice field will definitely make the atomic walking complicated in the small modulation frequency region. Strangely, when modulation frequency is small, the atomic walking around antinodes can stay unstable no matter how large the depth of the lattice is. When the frequency becomes higher, the stable region will expand and the walking is more preferred to a stable motion. According to Floquet's theory, the characteristic exponent μ of the trapping solution will be $\lim_{\omega \rightarrow \infty} \mu(0, -2\lambda/\omega^2) = 0$, which indicates a free atomic walking limit in a quickly varying lattice.

We should note here that the stable region of the real system Eq.(7) is not only vulnerable to the control parameters λ, ω but also heavily depends on the dynamic itself, i.e., the atom's position and momentum are also key parameters to determine the stability of atomic walking [38]. The nonlinear position-dependent of walking in Eq.(7) will introduce an effective part of \mathcal{E}_0 to shift the atom along the lattice, which actually breaks the spatial symmetry of the lattice walking. Naturally, an increase of atomic momentum will definitely reduce the stability region of the real trapping solution because the heated atom will more easily escape from the trapping region. The stable region of the linear solution indicates that the atom can surely be trapped in a shallow lattice field (small λ) with a higher modulation frequency ω .

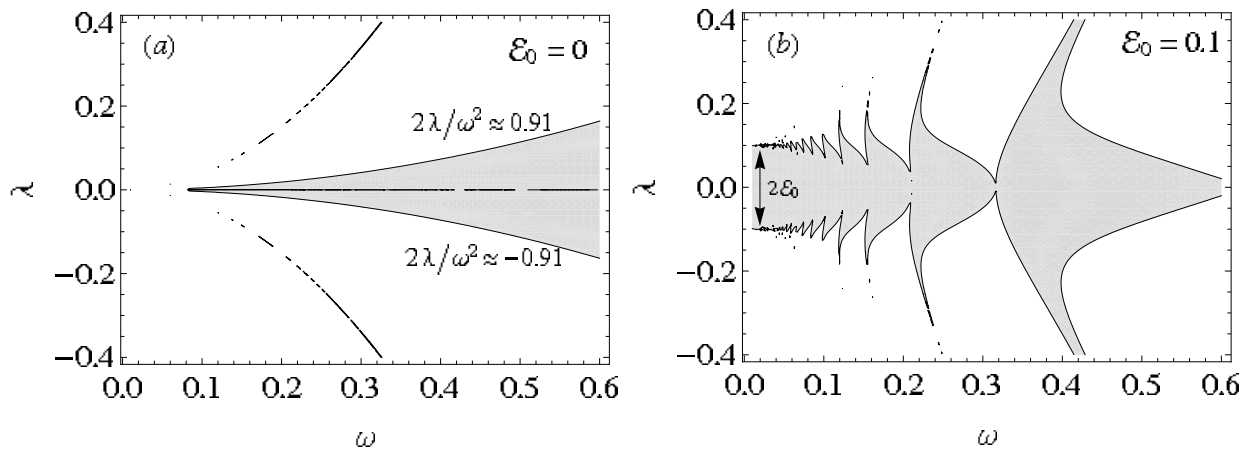


FIG. 8: The stability region for trapping state of linear solutions Eq.(17) in the $\lambda - \omega$ plane (a) for $\mathcal{E}_0 = 0$ and (b) for $\mathcal{E}_0 = 0.1$. The shaded area stands for the stable region.

D. Free ballistic flying

Finally, we consider two extreme conditions that the modulation frequency of the lattice is high ($\omega \gg \sqrt{\lambda}$) and the velocity of the atom is quick ($p \gg 2\sqrt{\lambda}$). For a large modulating frequency ω , the effective coupling constant meets $\lambda \cos(\omega t) \rightarrow 0$ and the equation can be simplified by

$$\ddot{x} \approx 0, \quad \omega \gg 1, \quad (18)$$

which means a negligible influence of light on atomic walking and implies a free flying of the atom in optical lattice, i.e., $x(t) \approx x(0) + p(0)t$ and $p(t) \approx p(0)$. In the other hand, when the speed of the atom is high, the atom also feels a quick oscillation of the force with a frequency of $p + \omega$ in one direction and $p - \omega$ in the opposite (see Eq.(8)). Both above cases are displayed in Fig.9(a) and Fig.9(b) by direct simulations of Eq.(7) where the thick black line, $x(t)$, indicate a nearly free flying motion and its slope is roughly determined by the initial momentum $p_0 \equiv p(0)$, showing a small relative change of atomic momentum during the walking process. The enlarged figures of the momenta between time interval $[0, 30]$ shown by the insets of Fig.9 demonstrate a beat oscillation of the atomic momentum around the initial value, with the average momentum satisfying $\langle p \rangle \approx p_0$. Therefore, the oscillation behavior can be approximately described by Eq.(8),

$$\frac{dp}{dt} = -\lambda \sin(p_0 t) \cos(\omega t),$$

and an integral of it gives

$$p(t) = p_0 + \frac{\lambda \cos[(p_0 - \omega)t]}{2(p_0 - \omega)} + \frac{\lambda \cos[(p_0 + \omega)t]}{2(p_0 + \omega)}, \quad (19)$$

which clearly reveals a beat oscillation of the momentum. Comparisons of solution Eq.(19) (the gray lines of the insets) with the strict solution (the black lines of the insets) are depicted in Fig.9(a) and Fig.9(b). The simulation indicates a good agreement of Eq.(19) with the strict Eq.(7) except for some minor differences. Besides, Eq.(19) also suggests a resonance behavior of the momentum when atomic momentum meets $p_0 \approx \pm\omega$. Under resonant condition, Eq.(19) becomes a bad approximation because the momentum will be divergent. However, as long as the condition of $\omega \gg \sqrt{\lambda}$ or $p_0 \gg 2\sqrt{\lambda}$ is satisfied, the momentum enhancement by the resonant effect in real system remains small relative to the large initial momentum, and the atom still keeps its ballistic flying under resonance condition. However, if the initial atomic momentum is small, this resonance effect will be manifest only under small modulation frequencies (see Eq.(19)) and this resonant behavior will also be suppressed by the nonlinear character of a real walking. Therefore, in conclusion, if the modulation frequency is high and the atomic momentum is large, the atom will almost conduct a free ballistic flying with its momentum taking a beat oscillation roughly around its initial value.

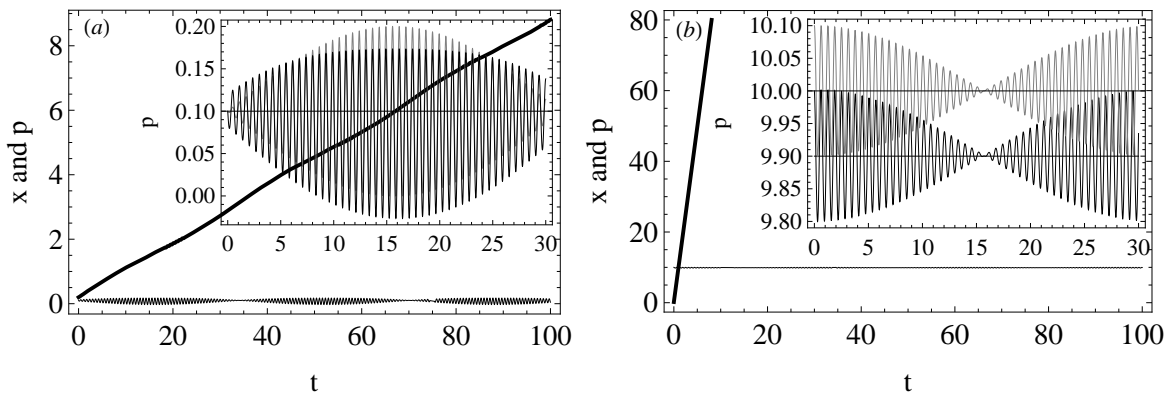


FIG. 9: The free flying of the atom (a) in a quickly varying field with $\omega = 10$, $p(0) = 0.1$, $x(0) = 0.2$, $\lambda = 1$ and (b) in a high speed under parameters $p(0) = 10$, $\omega = 0.1$, $x(0) = 0.2$, $\lambda = 1$. The insets are atomic momenta zoomed in between a time interval of $[0, 30]$ with the black lines for the strict equation and the grey ones for Eq.(19).

IV. CONCLUSIONS

A single atom coupled with high-finesse cavities is a fundamental system for quantum research, and many theoretical and experimental works have been done on this system [1–5, 34–36]. Directly based on quantum description, the quantum aspect of the dynamics are usually focused on, such as on nonclassical statistics, entanglement-induced effects, quantum information processing, which, contrarily, makes the classical contribution obscure. While some authors on this system concern more about the transmission of the light through a cavity to detect or control the atomic dynamics [34], such as detecting atomic trapping states, or controlling atomic trajectories [40, 41]. However all the atomic motion considered above are closely involved with the internal dynamic and the external dynamics is still mixing in atomic control. In order to investigate the external dynamic in a classical point of view, the internal variables should be decoupled or traced out. Raizen and his coworkers [42] resort to a dynamical map (periodic kicked rotator) based on pulsed standing field to investigate the atomic dynamic behavior and find a good agreement with the classical dynamic in a noisy environment. Particularly, their experiment studies on the motion of cold cesium atoms in an amplitude-modulated standing wave of light [29, 30] have a very close relation to our study in this paper. However, we use a simple classical model under a resonant condition and find a more rich dynamic behaviors of one atom in the optical lattice beyond a direct influence of internal dynamics.

As the fluctuating environment of the cavity mode, trapping a single atom in the cavity for a long time is turned out to be difficult. Therefore, sensitivity of the atomic motion to field modulation is a key problem for a practical one-atom control [30]. In this paper, we closely consider the classical walking of an atom in an field-controlled standing wave and reveals a diverse dynamic region of atomic motion. In the parametric region of lower modulation frequency, an oscillation with classical random jumping is found for cold atom. With the increasing of frequency, random atomic motion, chaotic transportation and the quasi-periodic trapping state appear. If the modulation frequency is high or the velocity of the atom in the lattice is large, the atom will exhibits a ballistic fly with a momentum beating oscillation. The study of dynamic stability shows that the transition between these dynamical regimes is irregularly determined not only by the lattice field but also by the position and momentum of the atom. Our results indicates a wide parametric region of unstable walking and a susceptibility of stable motion to the field fluctuations of amplitude and frequency as well as to the motion itself. Therefore, this work gives a rich clue for atomic control in the cavity and also provides a useful insight into the dynamical behavior of atoms in a periodically varying lattice.

Acknowledgements

This work is supported by the Shaanxi Provincial Natural Science Foundation (No.SJ08A12) and the National Science Foundation Project (No.10875076).

Appendix A: The derivation of Eq.(4)

The dynamic of atom in a certain field can be manipulated by different configuration of $\mathbf{E}(\mathbf{r}, t)$ according to the Hamiltonian of Eq.(2). A standing wave, generated by an interference of two quasi-monochromatic field with an envelop, $\mathcal{E}(\mathbf{r}, t)$, and the polarization, \mathbf{e}_λ , propagating in opposite direction, will be

$$\begin{aligned}\mathbf{E}(\mathbf{r}, t) &= \frac{1}{2}\mathbf{e}_\lambda\mathcal{E}(\mathbf{r}, t)[\cos(\nu t + \mathbf{k} \cdot \mathbf{r}) + \cos(\nu t - \mathbf{k} \cdot \mathbf{r})] \\ &= \mathbf{e}_\lambda\mathcal{E}(\mathbf{r}, t)\cos(\mathbf{k} \cdot \mathbf{r})\cos(\nu t),\end{aligned}$$

where ν is the carrier frequency and the slowly varying temporal envelop, $\mathcal{E}(\mathbf{r}, t)$, can be controlled in the experiment by changing the amplitude of the input field. If we stabilize the phase of the field in a linear cavity along x axis, the Hamiltonian of Eq.(3) will be got. More generally, we can write down the Schrödinger equation in the standing wave as

$$i\hbar\frac{\partial}{\partial t}\Psi(\mathbf{r}, t) = \left[\frac{\hat{p}^2}{2m} + \hat{H}_a - \Omega(\mathbf{r}, t)\cos(\nu t) \right] \psi(\mathbf{r}, t),$$

where

$$\Omega(\mathbf{r}, t) = \hat{\mathbf{d}} \cdot \mathbf{e}_\lambda \mathcal{E}(\mathbf{r}, t) \cos(\mathbf{k} \cdot \mathbf{r}),$$

and \hat{H}_a denotes the energy of the internal state: on ground state $|1\rangle$ with energy ϵ_1 , on excited state $|2\rangle$ with energy ϵ_2 . In real space, the atomic wavefunction can be written by a two-component form of

$$\Psi(\mathbf{r}, t) = \varphi_1(\mathbf{r}, t)e^{-i\epsilon_1 t/\hbar}|1\rangle + \varphi_2(\mathbf{r}, t)e^{-i\epsilon_2 t/\hbar}|2\rangle.$$

Under the rotating wave approximation, the Schrödinger equation for the two-component wave function is

$$\frac{\partial}{\partial t} \begin{pmatrix} \varphi_1 \\ \varphi_2 \end{pmatrix} = i \begin{pmatrix} \frac{\hbar}{2m}\nabla^2 & \Omega_R(\mathbf{r}, t)e^{-i\delta t} \\ \Omega_R(\mathbf{r}, t)e^{i\delta t} & \frac{\hbar}{2m}\nabla^2 \end{pmatrix} \begin{pmatrix} \varphi_1 \\ \varphi_2 \end{pmatrix}$$

where the detuning frequency $\delta = \omega_0 - \nu$ and the transition frequency $\omega_0 = (\epsilon_2 - \epsilon_1)/\hbar$. The Rabi frequency is defined by

$$\Omega_R(\mathbf{r}, t) = \frac{\Omega(\mathbf{r}, t)}{2\hbar} = \frac{\hat{\mathbf{d}} \cdot \mathbf{e}_\lambda}{2\hbar} \mathcal{E}(\mathbf{r}, t) \cos(\mathbf{k} \cdot \mathbf{r}).$$

In the experiment, the carrier frequency ν is adjusted to the transition frequency ω_0 (resonance $\delta = 0$), then

$$i\hbar\frac{\partial}{\partial t} \begin{pmatrix} \varphi_1 \\ \varphi_2 \end{pmatrix} = \begin{pmatrix} -\frac{\hbar^2}{2m}\nabla^2 & -\hbar\Omega_R(\mathbf{r}, t) \\ -\hbar\Omega_R(\mathbf{r}, t) & -\frac{\hbar^2}{2m}\nabla^2 \end{pmatrix} \begin{pmatrix} \varphi_1 \\ \varphi_2 \end{pmatrix}$$

In this case above equation can be decoupled by introducing [43]

$$\psi_+(\mathbf{r}, t) = \frac{1}{\sqrt{2}}[\varphi_1(\mathbf{r}, t) + \varphi_2(\mathbf{r}, t)], \quad \psi_-(\mathbf{r}, t) = \frac{1}{\sqrt{2}}[\varphi_1(\mathbf{r}, t) - \varphi_2(\mathbf{r}, t)],$$

with equations of

$$i\hbar\frac{\partial}{\partial t}\psi_+ = -\frac{\hbar^2}{2m}\nabla^2\psi_+ - \hbar\Omega_R(\mathbf{r}, t)\psi_+, \quad i\hbar\frac{\partial}{\partial t}\psi_- = -\frac{\hbar^2}{2m}\nabla^2\psi_- + \hbar\Omega_R(\mathbf{r}, t)\psi_-.$$

Above equation for wave functions $\psi_\pm(\mathbf{r}, t)$ indicates that the atom on any state will feel two different potentials

$$V_\pm(\mathbf{r}, t) = \mp\hbar\Omega_R(\mathbf{r}, t) = \mp\frac{\hat{\mathbf{d}} \cdot \mathbf{e}_\lambda}{2}\mathcal{E}(\mathbf{r}, t)\cos(\mathbf{k} \cdot \mathbf{r}).$$

If the envelop function of the field is controlled by (amplitude modulation field)

$$\mathcal{E}(\mathbf{r}, t) = g_0 \cos(\chi t),$$

the effective potential will be

$$V(\mathbf{r}, t) = \mp g_0 \frac{\hat{\mathbf{d}} \cdot \mathbf{e}_\lambda}{2} \cos(\chi t) \cos(\mathbf{k} \cdot \mathbf{r}) \equiv \hbar \lambda \cos(\chi t) \cos(\mathbf{k} \cdot \mathbf{r}).$$

For a linear cavity, the effective potential we pick up to consider is

$$V(x, t) = \hbar \lambda \cos(\chi t) \cos(kx),$$

where λ is the effective coupling parameter and χ is the modulation frequency of the field amplitude.

- [1] I. Teper, Yu-Ju Lin, and V. Vuletić, Phys. Rev. Lett. **97**, 023002 (2006).
- [2] A. Stibor, H. Bender, S. Kühnhold, J. Fortágh, C. Zimmermann and A. Günther, New J. Phys. **12**, 065034 (2010).
- [3] J. Ye, D. W. Vernooy, and H. J. Kimble, Phys. Rev. Lett. **83**, 4987 (1999).
- [4] S. Kuhr, W. Alt, D. Schrader, M. Mller, V. Gomer, D. Meschede, Science **293**, 278 (2001).
- [5] T. Wilk, S. C. Webster, A. Kuhn, G. Rempe, Science **317**, 488 (2007).
- [6] C. Monroe, Nature **416**, 238 (2002).
- [7] R. Arun, Offir Cohen, and I. Sh. Averbukh, Phys. Rev. A **81**, 063809 (2010).
- [8] S. R. Wilkinson, C. F. Bharucha, K. W. Madison, Qian Niu, and M. G. Raizen, Phys. Rev. Lett. **76**, 4512 (1996).
- [9] M. Karski, L. Förster, Jai-Min Choi, A. Steffen, W. Alt, D. Meschede, A. Widera, Science **325**, 174 (2009).
- [10] J. Jooa, P. L. Knight, J. K. Pachos, J. Mod. Opt. **54**, 1627 (2007).
- [11] S. Nie, S. R. Emory, Science **275**, 1102 (1997).
- [12] D. E. Chang, J. D. Thompson, H. Park, V. Vuletić, A. S. Zibrov, P. Zoller and M. D. Lukin, Phys. Rev. Lett. **103**, 123004 (2009).
- [13] F. L. Moore, J. C. Robinson, C. F. Bharucha, B. Sundaram, and M. G. Raizen, Phys. Rev. Lett. **75**, 4598 (1995).
- [14] A. C. Doherty, A. S. Parkins, S. M. Tan, and D. F. Walls, Phys. Rev. A **56**, 833 (1997).
- [15] P. Horak, G. Hechenblaikner, K. M. Gheri, H. Stecher, and H. Ritsch, Phys. Rev. Lett. **79**, 4974 (1997).
- [16] R. Graham, M. Schlautmann and P. Zoller, Phys. Rev. A **45**, R19 (1992).
- [17] In a real atomic-scale experiment, one atom can be traced and detected with a high resolution beyond the Heisenberg uncertainty principle.
- [18] D. M. Meekhof, C. Monroe, B. E. King, W. M. Itano, and D. J. Wineland, Phys. Rev. Lett. **76**, 1796 (1996).
- [19] V. Yu. Argonov and S. V. Prants, Phys. Rev. A **75**, 063428 (2007).
- [20] V. Yu. Argonov and S. V. Prants, Phys. Rev. A **78**, 043413 (2008).
- [21] S. V. Prants, JETP Lett. **75**, 777 (2007).
- [22] S. V. Prants, M. Edelman, and G. M. Zaslavsky, Phys. Rev. E **66**, 046222 (2002).
- [23] S. V. Prants and V. Yu. Sirotkin, Phys. Rev. A **64**, 033412 (2001).
- [24] F. Toscano, and D. A. Wisniacki, Phys. Rev. E **74**, 056208 (2006).
- [25] C. Gerry and P. Knight, *Introductory Quantum Optics*, Cambridge University Press, (Cambridge, 2005), Chap. 4.
- [26] A. R. Kolovsky, *Quantum chaos: double resonance model and its physical applications*, Lecture Notes in Physics **457**, 461 (1995).
- [27] Farhan Saif, Phys. Rep. **419**, 207 (2005).
- [28] P. L. Gould, G. A. Ruff, and D. E. Pritchard, Phys. Rev. Lett. **56**, 827 (1986).
- [29] D. A. Steck, W. H. Oskay, and M. G. Raizen, Science **293** 274 (2001).
- [30] D. A. Steck, W. H. Oskay, and M. G. Raizen, Phys. Rev. Lett. **88**, 120406 (2002).
- [31] F. L. Moore, J. C. Robinson, C. Bharucha, P. E. Williams, and M. G. Raizen, Phys. Rev. Lett. **73**, 2974 (1994).
- [32] D. B. Monteoliva, B. Mirbach, and H. J. Korsch, Phys. Rev. A **57**, 746 (1998).
- [33] L. E. Reichl, *The Transition to Chaos: Conservative Classical Systems and Quantum Manifestations*, 2nd ed, (Springer, NewYork, 2004).
- [34] P. Münstermann, T. Fischer, P. Maunz, P. W. H. Pinkse, and G. Rempe, Phys. Rev. Lett. **82**, 3791 (1999).
- [35] J. McKeever, J. R. Buck, A. D. Boozer, A. Kuzmich, H. C. Nägerl, D. M. Stamper-Kurn, and H. J. Kimble, Phys. Rev. Lett. **90**, 133602 (2003).
- [36] P. Domokos and H. Ritsch, Phys. Rev. Lett. **89**, 253003 (2002).
- [37] S. V. Prants and M. Yu. Uleysky, Phys. Lett. A **309**, 357 (2003).
- [38] G. Teschl, Ordinary Differential Equations and Dynamical Systems, Lecture Notes, <http://www.mat.univie.ac.at/gerald>.
- [39] A. Mouchet, C. Miniatura, R. Kaiser, B. Grémaud, and D. Delande, Phys. Rev. E **60**, 016221 (2001).
- [40] C. J. Hood, T. W. Lynn, A. C. Doherty, A. S. Parkins and H. J. Kimble, Science **287**, 1447 (2000).
- [41] T. W. Lynn, K. Birnbaum and H. J. Kimble, J. Opt. B: Quantum Semiclass. Opt. **7**, S215 (2005).
- [42] D. A. Steck, V. Milner, W. H. Oskay, and M.G. Raizen, Phys. Rev. E **62**, 3461 (2000).
- [43] R. J. Cook, Phys. Rev. Lett. **41**, 1788 (1978).